Polymer Chains in Confined Spaces and Flow-Injection Problems: Some Remarks

Takahiro Sakaue

Yukawa Institue for Theoretical Physics, Kyoto University, Kyoto 606-8502, Japan

Elie Raphaël*

Laboratoire de Physico-Chimie Théorique, UMR CNRS 7083,ESPCI, 10 rue Vauquelin, 75231 Paris Cedex 05, France

ABSTRACT: We revisit the classical problem of the behavior of an isolated linear polymer chain in confined spaces, introducing the distinction between two different confinement regimes (the *weak* and the *strong* confinement regimes, respectively). We then discuss some recent experimental findings concerning the partitioning of individual polymers into protein pores. We also generalize our study to the case of branched polymers, and study the flow-injection properties of such objects into nanoscopic pores, for which the strong confinement regime plays an important role.

I. Introduction

In recent years, much attention has been paid to the structure and dynamics of polymer chains in confined spaces.[1−3] For instance, understanding how biopolymers migrate through a narrow passageway to get to their targeted destination[4−8] is crucially important in cell biology.[9] In confined spaces, the number of available configurations for a polymer chain is reduced, leading to a free energy excess.[10] For an ideal linear chain confined in a space of characteristic size D (with $D < R_0$, where $R_0 = aN^{1/2}$ is the natural size of the chain, N is the number of monomers and a is the monomer size), this free energy excess was calculated by Cassasa:[11]

$$\frac{F_{id}}{k_B T} \simeq \left(\frac{R_0}{D}\right)^2 \tag{1}$$

(where $k_B T$ is the thermal energy).

Note that the scaling relation (1) holds equally for an ideal chain confined between two walls, in a cylindrical pore or in a spherical cavity. For a linear chain with excluded volume interactions, however, the confinement into a spherical cavity leads to an excess free energy that differs from the one corresponding to the confinement between two walls or in a cylindrical pore. Indeed, the nature of the confinement depends on whether the interactions between monomers become substantial or not in the confined state.

In the present article, we revisit these issues for various molecular architectures and propose to discriminate between two confinement regimes (depending on the geometrical nature of the confinement). In the first regime, called the *weak confinement regime* (WCR), the configuration of the polymer is restricted due to the confinement, but the conformation of the polymer at large length scale is still somewhat dilute. The free energy required for the confinement (measured from the unperturbed state in bulk) is of purely entropic origin and is an extensive function of the monomer number N. In the second regime, called the *strong confinement regime* (SCR), the chain is highly compressed and the confinement becomes stronger and stronger as the chain length increases. Here, the segmental

interactions dominate the entropic cost due to the confinement and, consequently, the free energy is no longer simply proportional to N. This departure of the excess free energy from a linear dependence on N was first noticed by Grosberg and Khokhlov[12] in the case of a linear polymer inside a closed cavity; unfortunately, this point is sometimes overlooked in the current polymer literature. We will show that for a linear chain, the SCR is only obtained in the case of a spherical cavity, while confinement between two walls or in a cylindrical pore corresponds to the WCR (sections II.A and II.B). We then discuss some recent experimental findings concerning the partitioning of poly(ethylene glycol) (PEG) molecules inside the protein pore[3,13−17] (section II.C). We next generalize our study to the case of polymers with arbitrary connectivity, using the concept of spectral dimension (section III). We show in particular that for a branched polymer, the SCR is already realized in a cylindrical pore. This is closely related to the notion of a "minimum diameter" for the capillary (introduced by Vilgis et al.[2,19]) and should be properly taken into account when one studies flow-injection problems[20,21] (section IV).

II. Linear Polymer in Confined Spaces

A. Linear Chain in the WCR Regime. Although in many practical cases the confinement geometry may be quite complicated, many fundamental features can be understood by considering simple geometries such as slits, capillaries, and spherical cavities. If a polymer chain is brought into such a confined space, the number of available spatial dimensions (which is $d = 3$ in bulk) is reduced at large scales. Hereafter, we will denote by d_c the number of "subtracted dimensions": at large length scales, the chain behaves as in a space of $d = 3 - d_c$ dimensions. For example, for a chain confined into a slit, one has $d_c = 1$. For the sake of simplicity, let us first consider the case of linear polymer. In dilute solution, its radius is given by[1]

$$R_3 = aN^{\nu_3} \tag{2}$$

where ν_3 is the Flory exponent (in a good solvent, $\nu_3 \simeq {}^3/_5$). If the chain is brought into a slit of diameter D ($d_c = 1$), its
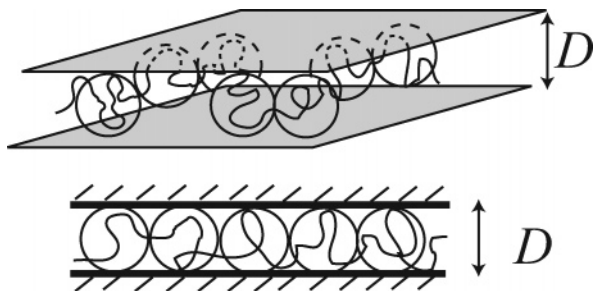
Figure 1. Drawing of a linear chain confined between a slit of width D (top) and inside a cylindrical pore of diameter D (bottom).
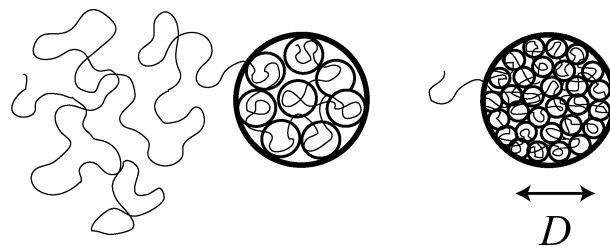

Figure 2. Drawing of a linear chain progressively confined inside a spherical cavity. As the confinement takes place, the monomer volume fraction inside the cavity increases and, consequently, the blob size decreases.

conformational behaviors depend on the ratio R_3/D. If $D < R_3$, the effect of confinement is important and the chain displays a two-dimensional behavior at length scales larger than D (Figure 1, top).[1,10] The polymer can be envisioned as a sequence of blobs of size D in the plane. The overall shape of the polymer is thus characterized by a thickness D and a radius R_2 given by[1]

$$R_2 \simeq D\left(\frac{N}{g}\right)^{\nu_2} \tag{3}$$

with ν_2 being the Flory exponent in two-dimension ($\nu_2 \simeq {}^3/_4$ in a good solvent condition). The number of segments in a blob g is given by

$$g \simeq \left(\frac{D}{a}\right)^{1/\nu_3} \tag{4}$$

Equation 4 means that inside blobs, the effect of wall is insignificant, thus, the internal correlations between segments are identical to those in bulk. From eqs 3 and 4, the radius of a linear chain confined in a slit is thus given by

$$R_2 \simeq aN^{\nu_2}\left(\frac{a}{D}\right)^{(\nu_2/\nu_3)-1} \tag{5}$$

Under good solvent conditions, the preceding equation yields

$$R_2 \simeq aN^{3/4}\left(\frac{a}{D}\right)^{1/4} \tag{6}$$

Now, let us consider the free energy per chain measured from the unperturbed state in bulk solution. As described above, the chain has to be reflected at the wall. For each collision, there exists a entropy cost of the order of thermal energy k_BT. Therefore, the free energy required for the chain confinement is easily evaluated as the entropy loss due to the confinement of N/g blobs:[1]

$$\frac{F_2}{k_BT} \simeq N\left(\frac{a}{D}\right)^{1/\nu_3} \tag{7}$$

Under good solvent conditions, one gets

$$\frac{F_2}{k_BT} \simeq N\left(\frac{a}{D}\right)^{5/3} \tag{8}$$

Note that the above confinement free energy can also be deduced from the following scaling argument:[1,10] (a) $F_2/(k_BT)$ is dimensionless and depends only on the length ratio R_3/D; (b) the leading term in $F_2/(k_BT)$ should be an extensive function of N. By imposing these two conditions, one indeed recovers eq 7.

A similar argument can be applied to the chain in a thin capillary (of diameter $D < R_3$), where the polymer shows one-dimensional ($d_c = 2$) behaviors at large length scale (Figure 1, bottom). Here, the chain can be envisioned as a succession of blobs of size D. At length scales larger than D, the chain shows one-dimensional conformational statistics, which results in

$$R_1 \simeq aN\left(\frac{a}{D}\right)^{(1/\nu_3)-1} \tag{9}$$

Thus, under good solvent conditions, we find

$$R_1 \simeq aN\left(\frac{a}{D}\right)^{2/3} \tag{10}$$

The free energy F_1 required to confine the chain inside the capillary is here again of order k_BT per blob, leading to

$$F_1 \simeq F_2 \tag{11}$$

(omitting numerical prefactors of order 1). In other words, the confinement free energy for a chain in a capillary obeys the same scaling law that for a chain in slit.

B. Linear Chain in the SCR Regime. Let us further decrease the number of available spatial dimensions by considering the behavior of a linear chain confined inside a spherical cavity ($d_c = 3$). Although sometimes adopted in recent publications, the assumption that the free energy has still the scaling form displayed by eq 7 is incorrect. This can be seen rather easily if one imagines the consequence of doubling the chain length (Figure 2).

For a chain in a slit or in a capillary, this does not affect the local properties at all, but just adds the same copy as the original system. Therefore, the free energy is proportional to N. However, for a chain in a spherical cavity, doubling the chain length inevitably increases the volume fraction of the chain. Therefore, the N dependence of the free energy should be stronger than linear.[12]

The scaling form for the free energy of a chain in a closed cavity F_0 of size D is deduced from the following thermodynamic requirements:[12] (a) $F_0/(k_BT)$ is dimensionless and depends only on the length ratio R_3/D; (b) $F_0/(k_BT)$ is extensive, that is to say, under the variable transformation $N \rightarrow kN$ and $\Omega (\simeq D^3) \rightarrow k\Omega$ (with $k > 0$), the free energy is modified as $F_0 \rightarrow kF_0$ (or equivalently, the pressure $P = -\partial F/\partial V$ remains unchanged). From these requirements, we obtain

$$\frac{F_0}{k_BT} \simeq \left(\frac{R_3}{D}\right)^{3/(3\nu_3-1)} \tag{12}$$

For a polymer chain in good solvent ($\nu_3 \simeq {}^3/_5$)

$$\frac{F_0}{k_BT} \simeq N^{9/4} \left(\frac{a}{D}\right)^{15/4} \tag{13}$$

Equation 12 can be rewritten by using the volume fraction of the chain $\phi \simeq Na^3/D^3$.

$$\frac{F_0}{k_BT} \simeq N\phi^{1/(3\nu_3-1)} \tag{14}$$

The free energy per segment depends only on the volume fraction, which indicates the analogy with semidilute polymer solutions. Along this line, it is possible to construct a blob picture for the chain confined in a spherical cavity. At short distances (smaller than the blob size ξ), the monomer–monomer correlations are similar to those in the bulk. The number g of monomers inside a blob is thus given by $\xi \simeq ag^{\nu_3}$. Moreover, the confined chain can be viewed as a compact stacking of blobs: $\phi \simeq ga^3/\xi^3$. From these two relations, the correlation length is found to be[12]

$$\xi \simeq a\left(\frac{D^3}{a^3N}\right)^{\nu_3/(3\nu_3-1)}$$

$$\simeq a\phi^{\nu_3/(1-3\nu_3)} \tag{15}$$

Under good solvent conditions, the correlation length thus decays as $N^{-3/4}$. The free energy can be estimated by using the k_BT per blob ansatz:

$$\frac{F_0}{k_BT} \simeq \frac{D^3}{\xi^3} \tag{16}$$

Substituting eq 15 into eq 16, one indeed recovers eq 12.

We see that there are two qualitatively different confinement regimes, depending on the confinement geometry. The threshold is obtained by calculating the volume fraction of the chain as a function of N

$$\phi = \frac{Na^3}{(R_d)^dD^{d_c}} \sim N^\alpha \tag{17}$$

where the exponent α is given by

$$\alpha = \frac{2(d_c-2)}{5-d_c} \tag{18}$$

If α is negative, as in the case of a chain confined into a slit (for which $\alpha = -{}^1/_2$), the confined chain is a rather dispersed system and its density decreases with chain length. We call such a regime the *weak confinement regime* (WCR). On the other hand, in the *strong confinement regime* (SCR), α is positive (as in the chain in a spherical cavity for which $\alpha = 1$); the confined chain is then reminiscent of a semidilute polymer solutions and its density increases with chain length. We see that a linear chain confined inside a cylindrical pore corresponds to the critical situation $\alpha = 0$; the overall chain is a dense packing of blobs, but its free energy is still given by that of the WCR (corresponding to entropy reduction). Note that this one-dimensional geometry corresponds to the lower critical dimension for a linear polymer, at which the chain is maximally stretched or equivalently $\alpha = 0$ (the volume fraction does not depend on N).

Let us end this section with several remarks:

(a) If a polymer is confined into the sphere of size

$$D^{min} \simeq aN^{1/3} \tag{19}$$

the volume fraction becomes unity. It means that it is physically impossible to confine the polymer into the sphere smaller than the minimum size D^{min}. The presence of minimum allowable size, which is much larger than the monomer size a, is a unique characteristic of the SCR. Various scaling formulas in SCR can be derived on the basis of D^{min} in a rather straightforward way. In the present case of a linear chain in the cavity, for instance, the correlation length is written in a scaling form as

$$\xi \simeq a\left(\frac{D}{D^{min}}\right)^p \tag{20}$$

The exponent p is determined from the requirement $\xi \to R_3$ at $D \to R_3$, leading to $p = 3\nu/(3\nu-1)$, which coincides with eq 15.

(b) In the case of the repulsive wall (no polymer adsorption), the monomer concentration should be reduced in the vicinity of the wall and become zero at the wall. The range of this monomer depletion is on the order of ξ. This leads to a surface energy

$$F_{surf} \simeq k_BTD^2/\xi^2 \simeq (D/a)^{2/(1-3\nu_3)} N^{2\nu_3/(3\nu_3-1)} \tag{21}$$

which is associated with the conformational entropy of the chain.[22] Under good and Θ solvent conditions, $F_{surf} \simeq k_BT(a/D)^{5/2}N^{3/2}$ and $F_{surf} \simeq k_BT(a/D)^4N^2$, respectively. The confinement free energy (eq 13) arising from segmental interactions is always larger than the surface energy.

(c) Self-consistent field theory results[23] show that the energy of a polymer chain confined in a sphere of radius D scales (for good solvent conditions) as $\sim a^3N^2/D^3$. Note that this last result—which is essentially a mean-field result—differs from our scaling prediction eq 13.[33]

(d) The behavior of confined polymer chains under Θ-solvent conditions (Flory exponent $\nu = {}^1/_2$) differs from those of ideal chains.[25] This is most manifest for strongly confined polymer chains. The free energy of a confined chain in a spherical cavity is given by

$$\frac{F_0{}^\theta}{k_BT} \simeq \left(\frac{a}{D}\right)^6N^3 \tag{22}$$

The N dependence is stronger than that in good solvent (eq 13). This is due to the fact that in a Θ solvent, the repulsive energy comes from the three-body interactions. More precisely, we predict the crossover of the scaling form $F_0/k_BT \sim N^{9/4}$ to $F_0/k_BT \sim N^3$ at high enough density. The onset of this crossover is derived by comparing the correlation length due to the confinement (cf. eq 15) with the thermal blob size $\xi_{th} \simeq a/\tau$, where $\tau \simeq (\Theta - T)/\Theta$ is the reduced temperature. With the effect of the slight attractive interaction, one can envision the chain conformation as the self-avoiding walk of thermal blobs at length scale smaller than the correlation length. By following the same argument as for the athermal case given above, one finds for the correlation length

$$\xi \simeq a\phi^{-3/4}\tau^{-1/4} \tag{23}$$

The excess free energy of the confinement is

$$\frac{F_0}{k_{\rm B}T} \simeq \left(\frac{a}{D}\right)^{15/4} N^{9/4} \tau^{3/4} \qquad (24)$$

When the confinement proceeds, or the solvent quality is reduced, this correlation length approach the thermal blob size and becomes equal at $\phi = \tau$. Above this point, the statistics inside the correlation blobs is Gaussian the confined chain is in the Θ condition regime. Then, the correlation length is given by

$$\xi \simeq a\phi^{-1} \qquad (25)$$

The corresponding free energy is given by eq 22

(e) Since the static behavior of a linear chain confined in a spherical cavity is reminiscent of a semidilute solution, we might expect that this analogy would also concerns some dynamical properties of the chain.

C. Partition Coefficient and Comparison with Experiment. The confinement free energy $F_{\rm c}$ (measured from the unperturbed state in a the bulk) is accessible experimentally by measuring the equilibrium partitioning of polymer molecules between the confined space and the bulk solution. The partition coefficient, p, is defined as the ratio of concentration between these two regions. The confinement free energy is then related to the partition coefficient through

$$p \simeq \exp\left(-\frac{F_c}{k_{\rm B}T}\right) \qquad (26)$$

For a linear chain in the presence of a slit, or of a cylindrical pore, the partition coefficient is obtained using the WCR confinement free energy (eq 7):

$$p \simeq \exp\left[-\left(\frac{R_3}{D}\right)^{1/\nu_3}\right] = \exp\left[-\left(\frac{a}{D}\right)^{1/\nu_3} N\right] \qquad (27)$$

In the case of a spherical cavity, on has to use the SCR confinement free energy (eq 12), leading to a partition coefficient:

$$p \simeq \exp\left[-\left(\frac{R_3}{D}\right)^{3/3\nu_3-1}\right] = \exp\left[-\left(\frac{a}{D}\right)^{3/(3\nu_3-1)} N^{3\nu_3/(3\nu_3-1)}\right] \quad (28)$$

In refs 13−15, the partitioning behaviors of poly(ethylene glycol) (PEG) molecules were investigated using single nanometer-scale pores formed by protein ion channels (see also ref 3). By monitoring the ionic conductance of a channel for various chain lengths, one can determine how the partition coefficient p varies as a function of N; using eq 26, one then obtains the behavior of the confinement as a function of chain length, $F_{\rm c}(N)$. From their experimental data, the authors of[13−15] conclude that the N-dependence of the free energy is sharper than predicted by theory. More precisely, the scaling theory for a linear chain confined in a cylindrical pore gives $F_{\rm c} \sim N$ (see eq 27), while the experimental data are well fitted by a relation of the form $F_{\rm c} \sim N^\mu$ with an exponent $\mu = 3.1 \pm 0.2$.

Let us remark, however, that the protein pore used in these experiments (*Staphylococcus aureus* α-hemolysin (α-toxin)) has following geometric characteristics (Figure 3).[3,18] The channel consists of a stem region and a large cap domain. In the cap domain, there is a pore entrance (approximately 2.6 nm in diameter). After that entrance, the diameter of the pore cross section gradually increases. After the widest part (approximately
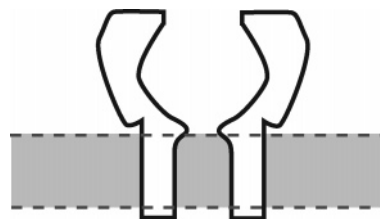

Figure 3. Schematic cross section of *S. aureus* α-hemolysin channel. For more detailed information based on X-ray studies, see refs 3 and 18.

3.6 nm in diameter), the diameter again decreases and reaches the narrowest constriction (approximately 1.5 nm in diameter), which is followed by the stem (approximated by cylindrical shape with average diameter of 2.2 nm).

Hence, if the polymer of size comparable to (or slightly larger than) the pore size enters the pore from the cis side (cap domain), it would be quite improbable for the polymer to negotiate the narrowest constriction, which effectively works as a geometric barrier. Taking account these features into account, it may be more favorable to model the protein pore as a (almost) closed cavity.

For a linear polymer confined inside a spherical cavity, we have seen that the free energy is given by eq 12. For good solvent conditions ($\nu_3 \simeq {}^3/_5$), we thus get $\mu = {}^9/_4$ (see eq 13), which is indeed much larger than the value $\mu = 1$ expected for a chain inside a cylindrical pore. The fact that the value of μ found experimentally ($\mu = 3.1 \pm 0.2$) is larger than ${}^9/_4$ might be due to the slight deviation from the perfect athermal assumption. As we have remarked in the last part of section II B, this leads to the crossover to the Θ solvent regime at high density ($\phi > \tau$), where one expects $\mu = 3$ in excellent agreement with experimental observations.

One should note, however, that other experiments suggest that the partitioning of PEG into a protein pore may be described by eq 27.[16,17] However, as mentionned by the authors, the data analyses for the cap domain are less convincing than those for the stem region, which is approximated by a cylindrical shape.

We also note the other recent experiment of relevance, where behaviors of fluorescently labeled single DNA molecules are observed within spherical cavities prepared by the colloidal templating method.[24] The results indicate the importance of segmental interactions, which is in accordance with our argument for the SCR.

In summary, the partitioning behaviors of flexible polymers into a nanoscale protein pore are not clear yet. Many experiments suggest that it may be important to take real geometry of the pore into account, and we hope that our remark may shed some light on the problem under dispute.

III. Confined Polymers with Arbitrary Connectivity

In the previous section, we restricted our attention to the linear polymers only. However, the behaviors of polymers with higher connectivity i.e., branched polymers, in confined space are also important. In this section, we extend the previous results to the case of polymeric fractal objects with arbitrary connectivity in a good solvent condition.

A. Criterion for the Confinement Regime. As can be speculated from the previous discussion on linear polymers, the borderline dimension between WCR and SCR for branched polymers will be given by the lower critical dimension of such objects. As we shall see below, the lower critical dimension of branched polymers is given by their spectral dimension. A simple and useful approach to confined branched polymers is a

Flory type of calculation, which allows us to obtain the spatial size of branched polymers in a given geometry.[2,19] First, let us define the notation in this section; N is the number of monomers in an arbitrary direction, M is the total number of monomers in a given polymer. These two quantities are related to so-called spectral dimension d_s:[26] $M = N^{d_s}$. The physical meaning of d_s would be recognized by checking some simple cases as followings: $d_s = 1$ corresponds to the simplest example of linear polymers, and $d_s = 2$ stands for a polymeric sheet. In more general cases, d_s is noninteger and statistically branched polymers correspond to $d_s \simeq 4/3$. Note that the spectral dimension depends on the connectivity (chemical structure of the cluster), but does not depend on the spatial conformation of the cluster. As for the previous section, d_c denotes the confining dimension (the number of subtracted dimension due to the confinement), D denotes the characteristic spatial size of the confinement geometry and R_d denotes the characteristic size of the polymer in d dimensional space: the usual Flory radius for $d = 3$, the radius of a pancake for $d = 2$ ($d_c = 1$), and the length of a cylinder for $d = 1$ ($d_c = 2$). Along with refs 2 and 19, we assume $d_s < 2$ in the following discussions.

Starting from the generalized Edwards Hamiltonian for the cluster with arbitrary connectivity, the corresponding mean-field Flory free energy is expressed as[2,19]

$$\frac{F}{k_BT} \simeq \frac{(R_3)^2}{a^2N^{2-d_s}} + \frac{a^3N^{2d_s}}{(R_3)^3} \qquad (29)$$

After minimization of the above equation with respect to R_3, one obtains the correct fractal dimension for polymers with arbitrary spectral dimension.

$$R_3 \simeq aN^{d_s+2/5} = aM^{d_s+(2/5)d_s} \qquad (30)$$

If the branched cluster is confined in $d = 3 - d_c$ dimensional space, the corresponding mean-filed Flory free energy is modified

$$\frac{F}{k_BT} \simeq \frac{(R_d)^2}{a^2N^{2-d_s}} + \frac{a^3N^{2d_s}}{D^{d_c}(R_d)^{3-d_c}} \qquad (31)$$

If the confining dimension d_c is smaller than the space dimension, the branched cluster finds a most preferable conformation in the restricted space. After minimization with respect to R_d, one obtains the optimum size[2,19]

$$R_d \simeq \left(\frac{a^5N^{d_s+2}}{D^{d_c}}\right)^{1/5-d_c} \qquad (32)$$

This leads to the volume fraction

$$\phi = \frac{N^{d_s}a^3}{(R_d)^{3-d_c}D^{d_c}} \sim M^{\alpha} \qquad (33)$$

where the exponent is

$$\alpha = \frac{2(d_s - 3 + d_c)}{(5 - d_c)d_s} \qquad (34)$$

Therefore, the critical confinement dimension is given by

$$d_c^* = 3 - d_s \qquad (35)$$

As we have already seen, for a linear polymer ($d_s = 1$), the

critical geometry corresponds to the capillary ($d_c = 2$). However, for branched polymers ($d_s > 1$), we encounter the SCR regime already in the capillary. Vilgis pointed out the presence of the minimum tube diameter D^{min} for branched polymers, which is, in fact, closely related to the SCR.[2,19] The volume fraction of the branched polymer confined in the capillary of size D^{min} becomes unity, thus, the capillary with the size $D < D^{min}$ is inaccessible to branched polymers. From eqs 32 and 33, it is found that

$$D^{min} = aM^{d_s-(1/2)d_s} \qquad (36)$$

For a linear polymer ($d_s = 1$), the minimum size of the capillary is equal to the monomer size as expected. However, for branched polymers with $d_s > 1$, the minimum size is much larger than the monomer size, and we notice once more that this is a unique characteristic of the SCR. Confined in the capillary with minimum diameter, the branched polymer assumes its maximally stretched state $R_1^{max} = aN = aM^{1/d_s}$, which is much smaller than the total length of the chemical path aM.

B. Confinement Free Energy of Polymeric Fractals. In this subsection, we give the confinement free energy of fractal objects with arbitrary connectivity beyond the mean-field approximation. The partition coefficient between a bulk and a confined space with a given geometry is obtained using eq 26.

Confinement in a Slit. From the previous subsection, fractal objects with ($1 \leq d_s < 2$) are weakly confined in a slit geometry. Therefore, the correlation length is set by the separation between slit D, and utilizing the usual scaling argument that the free energy should be proportional to the total polymerization index M, one obtains

$$\frac{F_2}{k_BT} \simeq \left(\frac{R_3}{D}\right)^2 \simeq \left(\frac{a}{D}\right)^2 M \qquad (37)$$

Confinement in a Capillary. In a narrow capillary, however, branched polymers with ($1 \leq d_s$) confined strongly. To calculate the corresponding free energy, it is convenient to apply the semidilute solution analogy, as described in section II.B in the case of linear polymers. A branched polymer inside the capillary is conceived as a dense piling of blobs of size ξ, which indicates the following relation

$$\frac{g}{\xi^3} \simeq \frac{M}{D^2R_1} \qquad (38)$$

with g being the number of monomers inside a blob. The streached length along the tube axis R_1 is deduced from eq 32;

$$R_1 \simeq \left(\frac{a^5M^{d_s+2/d_s}}{D^2}\right)^{1/3} \qquad (39)$$

Note that, as noticed in remark a, section II.B, a more clear-cut derivation of R_1 is possible through the scaling argument based on D^{min}: ($R_1 \simeq aN(D/D^{min})^{-2/3}$).

Inside a blob, the confinement is a weak perturbation, thus, the blob size ξ is related to the number of monomers g inside blob through eq 30;

$$\xi \simeq ag^{d_s+(2/5)d_s} \qquad (40)$$

From eqs 38−40, the blob size is deduced

$$\xi \simeq \left[\frac{D^{2(d_s+2)}}{a^{5(d_s-1)}M^{(d_s-1)(d_s+2)/d_s}}\right]^{(1/3)(3-d_s)} \qquad (41)$$

$$\simeq a\left(\frac{D}{D^{\min}}\right)^{2(d_s+2)/3(3-d_s)} \qquad (42)$$

For linear polymers ($d_s = 1$), one recovers the conventional result $\xi \simeq D$, i.e., blob size is set by the capillary size). However, for polymers with higher connectivity ($d_s > 1$), the correlation length decays with the increase in M. The confinement free energy is evaluated by assigning $\sim k_B T$ per blob;

$$\frac{F_1}{k_B T} \simeq \frac{D^2 R_1}{\xi^3} \simeq \left(\frac{R_3}{D}\right)^{10d_s/3(3-d_s)} \qquad (43)$$

$$\simeq \left(\frac{a}{D}\right)^{10d_s/3(3-d_s)} M^{2(2+d_s)/3(3-d_s)} \qquad (44)$$

For linear polymers ($d_s = 1$), one again rocovers the well-known result of eq 7, i.e., the free energy is proportional to the molecular weight.

Confinement in a Cavity. The free energy of branched polymers within a spherical cavity is obtained in a similar way. Now, one has to replace eq 38 by the following:

$$\frac{g}{\xi^3} \simeq \frac{M}{D^3} \qquad (45)$$

The blob size is given by

$$\xi \simeq \left(\frac{D^{3(d_s+2)}}{a^{5d_s}M^{d_s+2}}\right)^{(1/2)(3-d_s)} \qquad (46)$$

$$\simeq a\left(\frac{D}{D^{\min}}\right)^{3(d_s+2)/(3d_s+1)} \qquad (47)$$

where $D^{\min} = aM^{1/3}$ is the minimum allowable cavity size. By substituting $d_s = 1$, one recovers eq 15 with $\nu_3 = {}^3/_5$. One sees that the correlation length now decays with the increase in M even for linear polymers. For the confinement free energy, one finds

$$\frac{F_0}{k_B T} \simeq \frac{D^3}{\xi^3} \simeq \left(\frac{R_3}{D}\right)^{15d_s/2(3-d_s)} \qquad (48)$$

$$\simeq \left(\frac{a}{D}\right)^{15d_s/2(3-d_s)} M^{3(d_s+2)/2(3-d_s)} \qquad (49)$$

which is also deduced from the scaling argument (eq 12). By substituting $d_s = 1$, one recovers eq 13.

The extension to branched polymers with weak branching density is discussed in Appendix A.

IV. Injection of Polymeric Fractals into Narrow Capillaries

Up to now, our attention has been focused on equilibrium aspects of confined polymers. One important fact is that the partition coefficient shows a crossover behavior when the characteristic size of the confinement D becomes comparable to the natural size of the coil R_3 in a bulk. Although, as we already discussed, the sharpness of this crossover (dependence on the molecular weight) depends on the confinement regime, the common feature is that the probability to find the polymer in the space of $D < R_3$ is exponentially small.
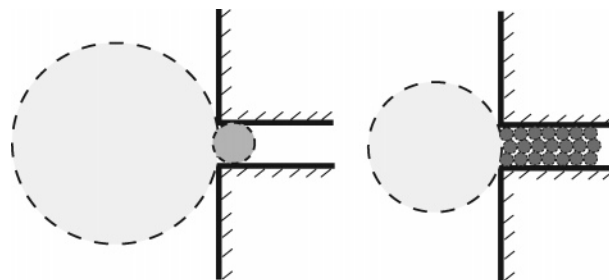

Figure 4. Schematic drawing of the penetration process of a polymeric fractal into narrow capillary. The branched polymer with $(1 < d_s)$ is progressively compressed with the penetration, consequently the blob size becomes smaller and smaller. The color strength represents the density.

However, it is possible to force the polymer into the space of size $D < R_3$ by applying certain flow, and the notion of SCR becomes much more evident here.[29] Aside from the fundamental interest, this is a subject of technological importance as a possible efficient methodology for the molecular characterization and separation.[21] This section is devoted to this problem of the forced injection of polymeric fractals into narrow space. The question of our interest is what is the minimum strength of solvent current J (measured as solvent flux inside the capillary) to achieve the polymer injection. One may naturally expect that the stronger current is necessary to inject larger branched polymers.[20,21] We demonstrate, however, this is indeed wrong.

Confined in the narrow capillary, the branched polymer is in a SCR. Therefore, the volume fraction of the branched polymer with $(1 < d_s)$ increases progressively with the penetration process advanced as is schematically shown in Figure 4. (Such a feature is, in fact, of a central importance in the present problem but is missed in the previous theory.) Suppose that a fraction of the branched polymer is already sucked inside the capillary (Figure 4). We denote the length of the capillary section occupied by the polymer as l, and the number of monomers sucked inside as P. To evaluate static structures of this polymer, one can follow the argument for the polymeric fractal in a capillary (section III.B), but now with the caution that our polymer is only partially injected. Therefore, two quantities l and P are related by eq 39 with the replacement of M by P.

$$l \simeq \left[\left(\frac{a^5}{D^2}\right)P^{d_s+2/d_s}\right]^{1/3} \qquad (50)$$

Instead of eq 42, the blob size is now dependent on l

$$\xi \simeq \left[\frac{D^{2(d_s+2)}}{a^{5(d_s-1)}P^{(d_s-1)(d_s+2)/d_s}}\right]^{(1/3)(3-d_s)} \qquad (51)$$

The number of monomer $g(l)$ inside a blob is related to $\xi(l)$ as the same relation for g and ξ (eq 40). Whether this polymer will be further injected or pushed back is in view of the balance between the osmotic force and the hydrodynamic drag force.

The osmotic force due to the confinement is

$$f_{osm} \simeq \Pi(l)D^2 \qquad (52)$$

where the osmotic pressure is given by $\Pi(l) \simeq k_B T/(\xi(l)^3)$. The hydrodynamic force is evaluated to be a sum of Stokes drag force per blob.

$$f_{hyd} \simeq \eta \xi(l)v\frac{P(l)}{g(l)} \qquad (53)$$

where the viscosity of the solvent is denoted as η and the velocity of the solvent inside a capillary is $v \simeq J/D^2$. By balancing these forces, we see that the current should be larger than some threshold $J_c^{(l)}$ to further inject the polymer:

$$\frac{\eta}{k_B T} J_c^{(l)} \simeq \left[\left(\frac{D}{a} \right)^5 P(l)^{-(2+d_s)/d_s} \right]^{2(2-d_s)/3(3-d_s)} \qquad (54)$$

This is a decreasing function of P (and, thus, l), which means that the more penetration process proceeds, the easier the pushing the branched polymer into a capillary is. The crucial moment is the injection of a first blob of size $\xi(D) = D$ (Figure 4 left), therefore, we reach the critical current

$$\frac{\eta}{k_B T} J_c = \frac{\eta}{k_B T} J_c^{(D)} \simeq 1 \qquad (55)$$

In contrast to our naive expectation that larger branched polymer would be injected into narrower capillary with more and more difficulties, the critical current neither on molecular size M nor the capillary size D, and noticeably it is the same as that for a linear polymer.[21,29] The key to capture this surprising result is the progressive nature of the confinement process and the growth rate of the two competing factors. The confinement force (eq 52) naturally increases with the permeation process advanced for polymers $d_s > 1$, but as can be seen easily, the flow induced driving force (eq 53) shows more rapid increase with l. Therefore, once the critical length of size D is inserted, the remaining part should be sucked in, and the cost to achieve the insertion of the primary blob does not depend on polymer specificity.

The extension to the case of weaker branching (cf. Appendix A) is straightforward, and one can show that critical current does not depend on both molecular size M and the degree of branching (in the notation of Appendix A, this is related to b), and again we are led to eq 55.

V. Conclusion

In the present article, we have revisited the problem of the behavior of a confined polymer chain and introduced the distinction between two confinement regimes. In the first regime, called the *weak confinement regime* (WCR), the confinement leads to a reduction of the configurational entropy of the chain. On the other hand, in the *strong confinement regime* (SCR), the chain becomes more and more compressed as its length increases, and, as a result, the dominant contribution to the confinement free energy arises from the intersegmental interactions. This leads to some unique features of the SCR: (i) progressive penetration process, (ii) nonlinear dependence of the confinement free energy on the segment number, (iii) local analogy with semidilute solutions, and (iv) existence of a minimum allowable size of the confinement. These features are closely related to each other, and the appearance of one of them is a manifestation of the SCR.

For a linear chain, the critical geometry separating the above-mentioned two regimes is the capillary tube. A linear chain confined in a closed cavity is thus in the SCR. We think that this may provide a possible interpretation of the recent experimental findings concerning the partitioning of PEG molecules into protein pores.[13–15] We would like to notice that the SCR for a linear chain is realized not only in the closed cavity but also in situations where a chain is intensely pressed by external force to the wall.[30]

We have developed similar arguments for branched polymers with arbitrary connectivity. We have shown in particular that branched polymers with spectral dimension $d_s > 1$ are in a SCR already when confined into a capillary. Using scaling arguments and a blob picture, we have analyzed some thermodynamic properties (like the confinement free energy and correlation length) of polymeric fractals in various confinement geometries.

We have also discussed the problem of forced injection of polymeric fractals into a narrow capillary. We have found that the critical current required for penetration depends neither on the molecular weight of the polymer nor on the capillary size. This result suggests that the simple forced permeation method discussed here will not be applicable in the context of the technological application (such as molecular characterization and separation). Nevertheless, we expect that by exploiting the nature of the SCR, it would be possible to construct an injection device which will enables us to probe the properties of branched structures.

Very recently, Nakaya et al. observed morphological changes in microemulsion droplets containing polymer chains.[31] We expect that the notion of the strong confinement discussed in the present paper plays a central role to interpret these experimental data.

Appendix A: Confined Branched Object: Case of Weaker Branching

In the main text, we assumed our branched polymer to be highly branched. However, there also exist branched polymers whose branching density is lower, i.e., there are substantial difunctional monomers between two adjacent branching point. In this appendix, we extend our discussion on the confined polymers to the case of weaker branching using one of the most important examples of polymeric fractals, i.e., *statistically branched polymer*. In terms of spectral dimension, statistically branched polymers are characterized by $d_s \simeq 4/3$. If one synthesizes branched polymers from the mixture of larger amount of difunctional monomers with multifunctional monomers, resultant products have lower branching density, then we denote the average number of such difunctional monomers between branching point as b. The natural size of such an object in a bulk solution is[28]

$$R_3 \simeq a M^{1/2} b^{1/10} \qquad (A1)$$

The case with $b = 1$ corresponds to the highly branched polymer. Note that by substituting $b = M$, we recover the usual coil size of linear polymers in good solvent.

Some modification for the free energy of confined branched polymer is necessary accordingly.

Chain in a Slit. In the slit problem, the modification is straightforward. From eq 37

$$\frac{F_2}{k_B T} \simeq \left(\frac{R_3}{D} \right)^2 \simeq \left(\frac{a b^{1/10}}{D} \right)^2 M \qquad (A2)$$

Chain in a Capillary. In this case, the modification is also straightforward if the diameter of the capillary is larger than some threshold $D^* = aM^{1/8}b^{19/40}$.[20,21] All we have to care about is that now the blob size ξ is related to the number of monomers inside g as

$$\xi \simeq ag^{1/2}b^{1/10} \tag{A3}$$

instead of eq 40. Then, the correlation length is

$$\xi \simeq \left(\frac{D^4}{R_3}\right)^{1/3} \simeq \frac{D^{4/3}}{a^{1/3}M^{1/6}b^{1/30}} \quad (D > D^*) \tag{A4}$$

and the confinement free energy is

$$\frac{F_1}{k_BT} \simeq \frac{D^2R_1}{\xi^3} \simeq \left(\frac{R_3}{D}\right)^{8/3} \tag{A5}$$

$$\simeq \left(\frac{ab^{1/10}}{D}\right)^{8/3} M^{4/3} \quad (D > D^*) \tag{A6}$$

All of these results coincide with those in the previous subsection if the distance between branching points is unity ($b = 1$). We call such a situation ($D > D^*$) as regime I.[34]

However, if the capillary becomes narrower ($D < D^*$), additional considerations are necessary, since, then, the blob size ξ (eq A4) becomes smaller than the characteristic spatial size of linear segment between branching points $\simeq ab^{3/5}$.[20,21] In such a case (called regime II), the confined branched object locally looks like semidilute solution of linear polymers, where instead of eq A3, the relation $\xi \simeq ag^{3/5}$ is expected. Therefore, the correlation length and the confinement free energy are, respectively, deduced as

$$\xi \simeq D\left(\frac{b}{M}\right)^{1/8} \quad (D < D^*) \tag{A7}$$

$$\frac{F_1}{k_BT} \simeq \frac{D^2R_1}{\xi^3}e\left(\frac{R_3}{D}\right)^{5/3}\left(\frac{M}{b}\right)^{3/8} \tag{A8}$$

$$\simeq \left(\frac{a}{D}\right)^{5/3}\frac{M^{29/24}}{b^{5/24}} \quad (D < D^*) \tag{A9}$$

By replacing b by M in these results in regime II, we recover results for a linear polymer in the capillary ($\xi = D$ and eq 7).

Chain in a Spherical Cavity. The situation is the same as that in the capillary problem. The correlation lengths in regime I and regime II are derived in a similar way as in the capillary problem, which are respectively written as

$$\xi \simeq \frac{D^3}{R_3^2} \simeq \frac{D^3}{a^2Mb^{1/5}} \quad (D > D^*) \tag{A10}$$

$$\xi \simeq \left(\frac{D}{a}\right)^{5/4}\frac{D}{M^{3/4}} \quad (D < D^*) \tag{A11}$$

where the crossover cavity size is $D^* \simeq aM^{1/3}b^{4/15}$. Therefore, the confinement free energies in these regimes are respectively

$$\frac{F_0}{k_BT} \simeq \left(\frac{R_3}{D}\right)^6 \tag{A12}$$

$$\simeq \left(\frac{a}{D}\right)^6 b^{3/5} M^3 \quad (D > D^*) \tag{A13}$$

$$\frac{F_0}{k_BT} \simeq \left(\frac{a}{D}\right)^{15/4} M^{9/4} \quad (D < D^*) \tag{A14}$$

Both results of correlation length and free energy in regime II do not depend on b, and they coincide with those for a linear polymer in a cavity (eq 15 with $\nu_3 = \frac{3}{5}$ and 13).

References and Notes

(1) de Gennes, P.-G. *Scaling Concepts in Polymer Physics*; Cornell University Press: Ithaca, NY, 1979.
(2) Vilgis, T. A. *Phys. Rep.* **2000**, *336*, 167.
(3) *Structure and Dynamics of Confined Polymers*; Kasianowicz, J. J., et al. Eds.; Kluwer Academic Publishers: Dordrecht, The Netherlands, 2002.
(4) Kasianowicz, J. J.; Brandin, E.; Branton, D.; Deamer, D. W. *Proc. Natl. Acad. Sci. U.S.A.* **1996**, *93*, 13770.
(5) Lubensky, D. K.; Nelson, D. R. *Biophys. J.* **1999**, *77*, 1824.
(6) Muthukumar, M. *Phys. Rev. Lett.* **2001**, *86*, 3188.
(7) Meller, A.; Nivon, L.; Branton, D. *Phys. Rev. Lett.* **2001**, *86*, 3425.
(8) Chuang, J.; Kantor, Y.; Kardar, M. *Phys. Rev. E* **2002**, *65*, 11802.
(9) Alberts, B.; Johnson, A.; Lewis, J.; Raff, M.; Roberts, K.; Walter, P. *Molecular Biology of the Cell*, 4th ed.; Garland Publishing: New York, 2002.
(10) Daoud, M.; de Gennes, P.-G. *J. Phys. (Paris)* **1977**, *38*, 85.
(11) Cassasa, E. F. *J. Polym. Sci.* **1967**, *B5*, 773.
(12) Grosberg, A. Yu.; Khokhlov, A. R. *Statistical Physics of Macromolecules* American Institute of Physics: New York, 1994.
(13) Bezrukov, S. M.; Vodyanoy, I.; Brutyan, R. A.; Kasianowicz, J. J. *Macromolecules* **1996**, *29*, 8517.
(14) Merzlyak, P. G.; Yuldasheva, L. N.; Rodriques, C. G.; Carneiro, C. M. M.; Krasilnikov, O. V.; Bezrukov, S. M. *Biophys. J.* **1999**, *77*, 3023.
(15) Rostovtseva, T. K.; Nestorovich, E. M.; Bezrukov, S. M. *Biophys. J.* **2002**, *82*, 160.
(16) Movileanu, L.; Bayley, H. *Proc. Natl. Acad. Sci. U.S.A.* **2001**, *98*, 10137.
(17) Movileanu, L.; Cheley, S.; Bayley, H. *Biophys. J.* **2003**, *85*, 897.
(18) Deamer, D. W.; Branton, D. *Acc. Chem. Res.* **2002**, *35*, 817.
(19) Vilgis, T. A.; Haronska, P.; Benhamou, M. *J. Phys. II* **1994**, *4*, 2187.
(20) Gay, C.; de Gennes, P.-G.; Raphaël, E.; Brochard-Wyart, F. *Macromolecules* **1996**, *29*, 8379.
(21) de Gennes, P.-G. *Adv. Polym. Sci.* **1999**, *138*, 92.
(22) Lifshitz, I. M.; Grosberg, A. Yu.; Khokhlov, A. R. *Rev. Mod. Phys.* **1978**, *50*, 683.
(23) Kong, C. Y.; Muthukumar, M. *J. Chem. Phys.* **2004**, *120*, 3460.
(24) Nykypanchuk, D.; Strey, H. H.; Hoagland, D. A. *Macromolecules* **2005**, *38*, 145.
(25) Raphael, E.; Pincus, P. *J. Phys. II* **1992**, *2*, 1341.
(26) Alexander, S.; Orback, R. *J. Phys., Lett.* **1982**, *43*, L625.
(27) Isaacson, J.; Lubensky, T. C. *J. Phys., Lett.* **1980**, *41*, L649.
(28) Daoud, M.; Joanny, J.-F. *J. Phys.* **1981**, *42*, 359.
(29) Sakaue, T.; Raphaël, E.; de Gennes, P.-G.; Brochard-Wyart, F. *Europhys. Lett.* **2005**, *72*, 83.
(30) Sakaue, T. *DNA electrophoresis in designed channels*, arXiv: cond-mat/0509403, to appear in *Eur. Phys. J. E.*
(31) Nakaya, K.; Imai, M.; Komura, S.; Kawakatsu, T.; Urakami, N. *Europhys. Lett.* **2005**, *71*, 494.
(32) Cacciuto, A.; Luijten, E. *Nano Lett.* (Published on Web 01/24/2006).
(33) Very recent Monte Carlo simulations[32] have unambiguously shown that the confinement free energy is consistent with our scaling prediction.
(34) In ref. 20, regime I and regime II (see below) were called weak and strong confinement, respectively. However, it should be noticed that the meaning of these terminologies is different from the concept in our present discussion on the nature of polymer confinement.